

REPORT DOCUMENTATION PAGE

Form Approved OMB No. 0704-0188

Public reporting burden for this collection of information is estimated to average 1 hour per response, including the time for reviewing instructions, searching existing data sources, gathering and maintaining the data needed, and completing and reviewing the collection of information. Send comments regarding this burden estimate or any other aspect of this collection of information, including suggestions for reducing this burden to Washington Headquarters Services, Directorate for Information Operations and Reports, 1215 Jefferson Davis Highway, Suite 1204, Arlington, VA 22202-4302, and to the Office of Management and Budget, Paperwork Reduction Project (0704-0188), Washington, DC 20503.

1. AGENCY USE ONLY (Leave blank)		2. REPORT DATE 07-March-2001	3. REPORT TYPE AND DATES COVERED Final Report	
4. TITLE AND SUBTITLE Applications of Superconductivity to Hall Thrusters Propulsion			5. FUNDING NUMBERS F61775-00-WE038	
6. AUTHOR(S) Professor Claudio Bruno				
7. PERFORMING ORGANIZATION NAME(S) AND ADDRESS(ES) University of Rome Via Eudossiana 18 Rome 00184 Italy			8. PERFORMING ORGANIZATION REPORT NUMBER N/A	
9. SPONSORING/MONITORING AGENCY NAME(S) AND ADDRESS(ES) EOARD PSC 802 BOX 14 FPO 09499-0200			10. SPONSORING/MONITORING AGENCY REPORT NUMBER SPC 00-4038	
11. SUPPLEMENTARY NOTES				
12a. DISTRIBUTION/AVAILABILITY STATEMENT Approved for public release; distribution is unlimited.			12b. DISTRIBUTION CODE A	
13. ABSTRACT (Maximum 200 words) This report results from a contract tasking University of Rome as follows: The contractor will investigate the use of superconducting materials for use in high power hall effect type electric propulsion motors. The focus of this work will be to derive scaling laws for coils using high temperature superconducting materials in a Hall SPT up to 50 kW electric power. The contractor will compare the results of this system to more traditional thrusters and discuss the performance gains/limitations. He will collect all data and findings and write a final report.				
14. SUBJECT TERMS EOARD, Electric Propulsion, Superconductivity, Hall effect thrusters			15. NUMBER OF PAGES 25	16. PRICE CODE N/A
17. SECURITY CLASSIFICATION OF REPORT UNCLASSIFIED	18. SECURITY CLASSIFICATION OF THIS PAGE UNCLASSIFIED	19. SECURITY CLASSIFICATION OF ABSTRACT UNCLASSIFIED	20. LIMITATION OF ABSTRACT UL	



University of Rome "La Sapienza"

Rome, Italy

Superconducting Materials Applied to EP Systems

C. Bruno, D. Casali

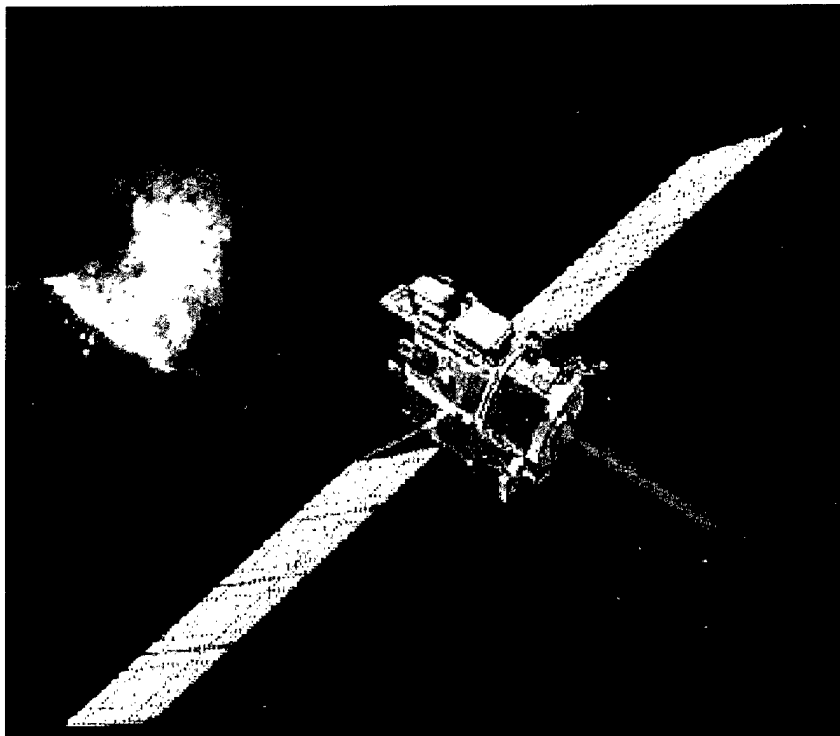
University of Rome "La Sapienza"

Dept. of Mechanics and Aeronautics

Via Eudossiana, 18

00184 Rome

Italy



20010806 101

AQ FOI-11-2184

Table of Contents

1 – Introduction.....	1
2 - Superconducting materials.....	2
3 - Applying of SC materials to EP systems; benefits.....	4
4 - Low power scaling of SC coils – equipped Hall thrusters.....	9
5 - Stresses on magnetic coils.....	12
6 - Cooling systems for SC coils.....	15
7 – Specific development topics.....	18
7.1 Plume divergence.....	18
7.2 B fields interference.....	18
8 - Overview for future applications.....	19
8.1 Low Power Hall Thrusters.....	19
8.2 High Power Hall Thrusters.....	20
8.3 MPD Thrusters.....	21
8.4 Conclusions.....	22
References.....	23

SUPERCONDUCTING MATERIALS APPLIED TO EP SYSTEMS

C. Bruno, D. Casali
University of Rome "La Sapienza"
Dept. of Mechanics and Aeronautics
Via Eudossiana, 18
00184 Rome, Italy

1 - Introduction

In recent years interest in EP systems has grown, due to their potential for space propulsion. Activities and programs about EP systems are undertaken in Europe, USA and Japan. Comparing EP systems performance (in terms of I_{sp}) to that of classical chemical thrusters, it can be seen that while the latter have I_{sp} in the range of 300 ÷ 500 s, the former have I_{sp} in the range of 400 ÷ 8000 s. This means, for a given mission, a dramatic reduction in propellant consumption. Figure 1 reports I_{sp} for different propulsion systems.

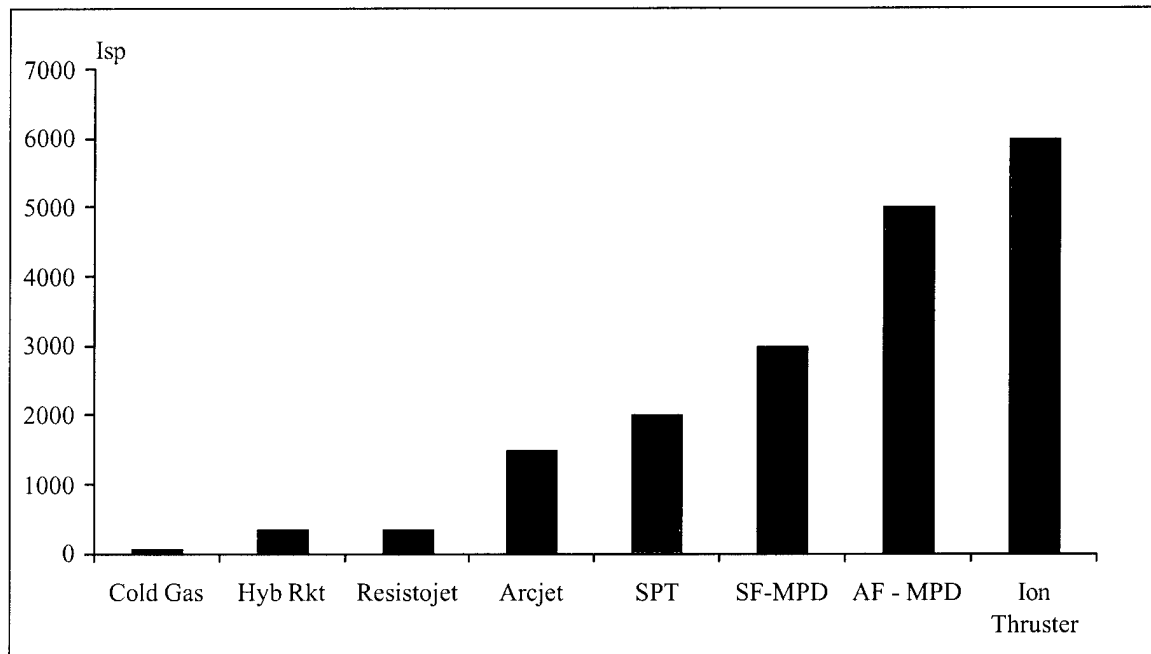


Figure 1: I_{sp} for different propulsion systems

The propellant savings using EP can be exploited to increase the payload mass or to achieve the same mission with smaller and less expensive launch vehicles. In figure 2 the propellant total weight / satellite total weight is reported for a satellite total weight of 2400 Kg, changing orbit from 250 Km to G.E.O. [Giucci, 1999].

Another advantage in using EP systems instead of chemical thrusters, is their highly controllable thrust, which makes EP the ideal system for attitude control, stationkeeping and orbit adjustment.

On the other side, an EP system needs considerable electrical power to produce high I_{sp} and efficiency. This implies a mass penalty (mostly due to solar panels and PCU). The limits imposed by the electrical power system are reflected in the maximum thrust available ($F = JxB$), which is of the

order of mN to N (depending on applications). To overcome such problems Superconducting (SC) materials can be exploited.

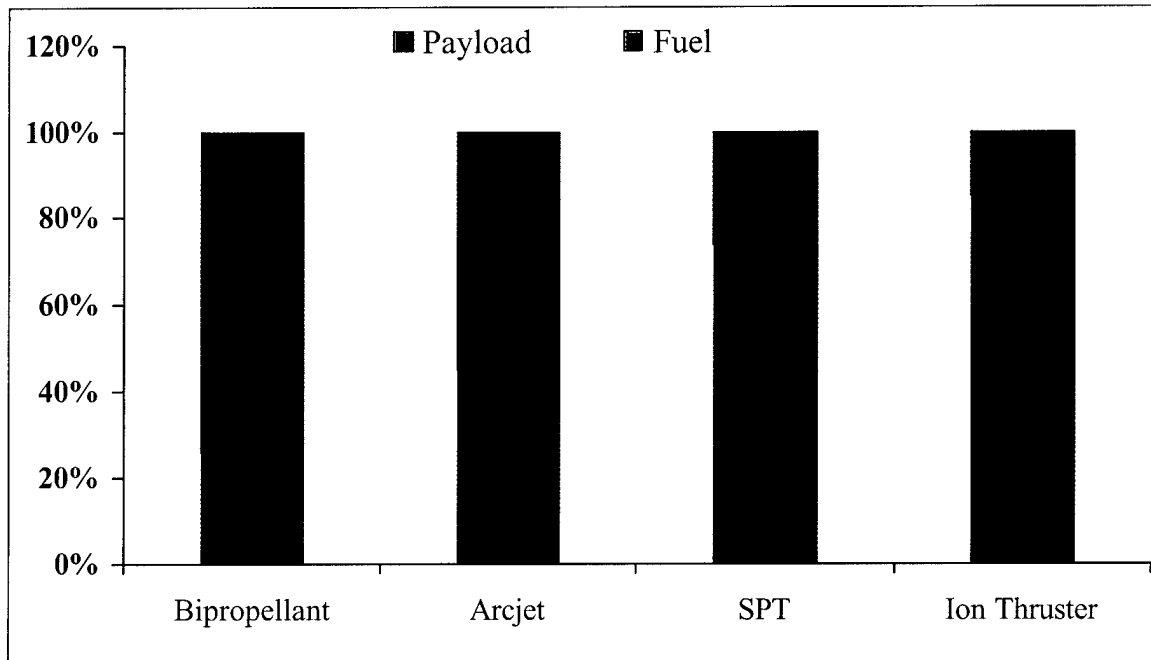


Figure 2: Weight distribution for different propulsive systems [Giucci, 1999]

2 - Superconducting materials

Superconductivity is a property of a material for which resistivity and magnetic permeability is close to or nearly zero. Superconductivity is well explained by the BCS theory (developed by J. Bardeen, L. N. Cooper and J. R. Schiffer): in a material in the superconductive state, conducting electrons propagate through without any resistance, because they form a moving pair (Cooper's pair); the creation of Cooper pairs is due to the interaction of the electrons with the mechanical vibrations of the crystalline reticulated structure; the atoms vibrations in the reticulated structure tend to diminish the repulsive force among electrons, a phenomenon equivalent to produce an attractive force between the electrons pair. The intensity of this interaction depends strongly on temperature. The temperature for which a material switch from SC to NC state is the "critical" or "transition" temperature. Second important feature of SC material is the capacity of expelling a magnetic flux (self induced or applied): this characteristic is known as the Meissner effect.

Two important microscopic reference length have been determined for SC material:

- Coherence length: this is the space distance between two electrons in a Cooper's pair.
- if a magnetic field is applied to a SC material, the field does not drop abruptly to zero, but there is a characteristic decay length, called London penetration depth

Based on these reference length, SC materials can be classified as follows:

- Type I SC.
- Type II SC.

Type I SC materials are characterized by a coherence length greater than the penetration depth; these become SC materials under the following conditions: low transition temperature ($5 \div 10$ K)

and low intensity magnetic fields. If one of the two conditions is not met, the superconducting state disappears. Such materials are of academic interest, but rarely used in applications.

More interesting, from a technological point of view, are type II SC materials; these are characterized by a penetration depth greater than the coherence length; therefore they can remain superconductive at high magnetic field intensity, i.e., until the so called upper critical field, therefore carrying more intense currents.

Inside the type II SC materials, a new family of superconductors has been discovered: these are copper oxide ceramics, (e.g., YBCO, a Yttrium, Barium and Copper Oxide ceramic), characterized by having higher transition temperature (>120 K; High Temperature Super Conducting materials = HTSC) compared to ordinary type II SC materials having "low" transition temperature ($20 \div 25$ K: Low Temperature Super Conducting materials = LTSC). This feature initially seemed to make oxide ceramics the ideal material for SC application, but it was discovered that in high magnetic fields (magnetic fields of technological interest can be as high as 40 T) the material resistivity becomes up to 100 times that of a NC material (e.g., Cu), unless the temperature was lowered to $20 \div 30$ % of the transition value. The reason for this behavior is nowadays explained as follows: when high currents are applied to a SC material, the magnetic field is present in form of flux tubes

(fluxoids) inside the material. While in a LTSC material the fluxoids are arranged in a rigid triangular reticulated structure, in a HTSC their structure is disordered and aggregated (the so called liquid of vortices). Now when a current flowing in the HTSC material interacts with the one around the fluxoid, a force (Magnus force) is created and exerted on the fluxoid, forcing it to move in a direction perpendicular to both the current and the fluxoid. In this way energy is dissipated, which induces a potential difference and, therefore, an equivalent resistivity in the material. This phenomenon is a limit to the current that can flow in the material without destroying its superconducting state; in any case SC materials can stand currents of the order of thousands of A/mm², far beyond that of NC materials.

To fully exploit HTSC materials without having to lower the temperature, defects or impurities are purposely inserted in the material; these imperfections work as obstacles (pinning forces) for the fluxoid, preventing its motion in the material, and reducing resistivity.

Although the appealing properties, HTSC materials show a major problem which, in first instance could be an obstacle in the development of longer wires and tapes for electric power devices; in fact the polycrystalline compounds, of which HTSC materials are made of, usually consist of multiple grains whose boundaries reduce the supercurrent flow. An answer to this problem could be the doping of material: if, for example, YBCO is to be considered as HTSC material, Yttrium ions (Y^{3+}) could be replaced by Calcium ions (Ca^{2+}), being almost identical in size. Studies in this field [Hammerl et al, 2000], have shown that Calcium doping leads to strongly enhanced current densities values at low temperatures (< 77 K). At 77 K, however, the critical current densities are not significantly increased; this is due to the fact that if the grains, as well as the boundaries, receive the same amount of Ca^{2+} , the former result is over-doped; as a consequence there is a reduction for the material critical temperature T_c . A solution to this problem consists in over-doping the grain boundaries, while keeping the grains optimally doped. This can be achieved growing a calcium-doped YBCO film over an undoped one: using this technique in their latest work, Hammerl et al., have found that some of the Ca^{2+} appears to migrate into the grain boundaries, partially healing them. Figure 3 shows the behavior of the material in terms of current densities vs. temperature for an undoped material, for a "generic" doped material and for "targeted" doped materials.

Research and development in the HTSC technology have been and still are performed by major industries, such as Pirelli Cables and Systems Company, where testing and commercial production of HTSC cables are under way.

Programs for application of SC materials to propulsion systems are under way as well; a research group [Prof. Negrini Francesco et al.] at University of Boulogne, Italy, has developed a code for the optimized design of superconducting coils. In particular this code has been used for the design of magnetic coils for MHD applications [www.die.ing.unibo.it].

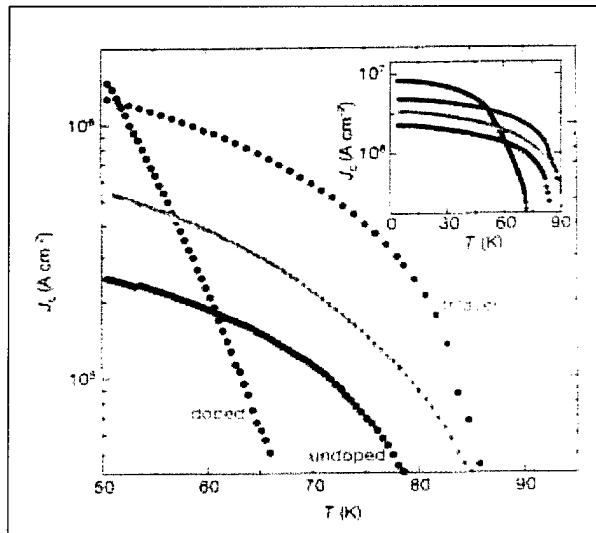


Figure 3: Behavior of the material in terms of current densities vs. temperature [Hammerl et al.]

3 - Applying of SC materials to EP systems; benefits

Applications of SC materials to EP systems can lead to serious benefits in terms of weight and volume savings. Early studies [D. J. Connolly et al., 1971] have shown how the replacing a conventional magnet with a superconducting magnet in a MPD thruster could improve performance and efficiency. In the next figure the performance of a superconducting magnet MPD thruster with hollow cathode and argon propellant is reported.

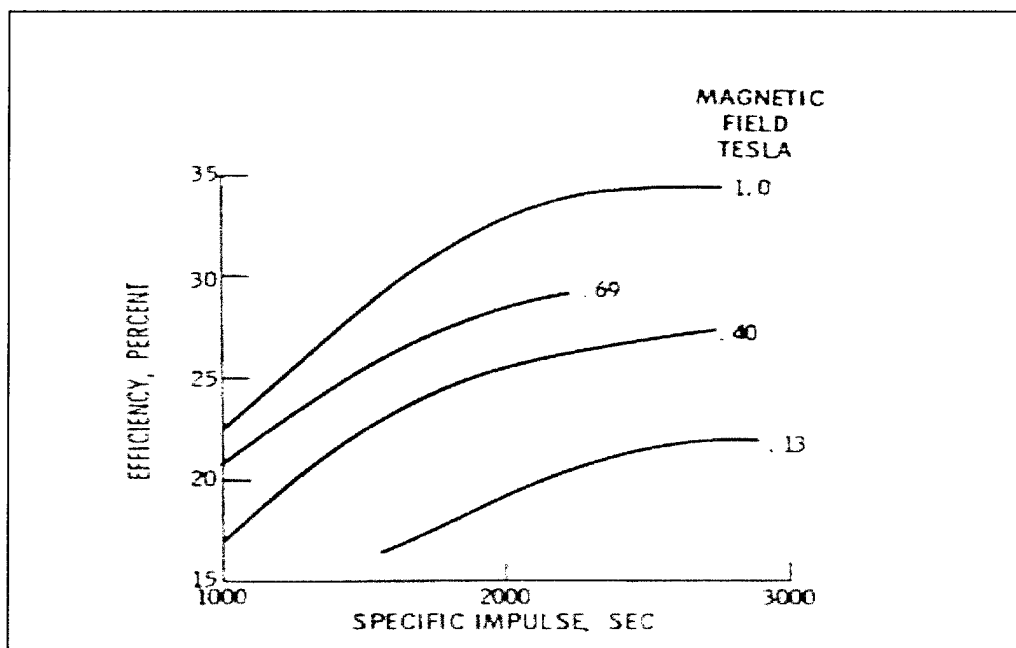


Figure 4: Performance and efficiency of a MPDT with superconducting magnet [D. J. Connolly et al., 1971]

At temperatures less than the critical value, SC materials have resistivity and permeability values close to zero; these features make SC materials ideals for EP thrusters: currents flowing in the material do not need a voltage (and power!) to be maintained; at zero resistivity a starter circuit creates them, after which they keep circulating (almost) indefinitely. Magnetic fields can therefore be created without ohmic losses. The possibility of having high currents density, implies high B fields, which are exploited in terms of Lorentz thrust ($F= J \times B$); for a specific mission this means a reduction in coil power requirements and weight [Reed and Sovey, 1988].

SC materials can be utilized for AF – MPDT and Hall Thrusters (HT): in these propulsion systems the electric coil needed to generate a magnetic field could be made of SC instead of NC material. Noting that the number of turns in a coil is inversely proportional to current densities, it is easy to see how the use of SC materials lead to an improvement in volume saving.

To see the benefits of employing SC instead of a NC material (Cu), we considered a coil, applied to a MPDT, having the following features:

- Length: $L = 0.1$ m
- Diameter: $D = 0.14$ m
- Wire diameter: $d_w = 1$ mm

The following tables report the results of calculations performed at DMA [Giucci, 1999] for copper and for a type II SC material (NbTi), varying the B field in the range of 0.1 – 0.6 T: this is an interesting B range for current (typical) EP satellite applications.

B field	T	0.05	0.1	0.2	0.3	0.4	0.5	0.6
Current density	A/mm ²	10	10	10	10	10	10	10
Total wire length	m	637	1273	2546	3820	5093	6366	7639
Total wire resistance	Ohm	13.78	27.56	55.12	82.68	110.24	137.8	165.36
Required power	W	850	1700	3400	5100	6800	8500	10200
Total wire weight	Kg	4.465	8.930	17.860	26.790	35.720	44.650	53.580
Winding layers		15	29	58	87	116	145	174

Table 1: Coil characteristics for copper winding

B field	T	0.05	0.1	0.2	0.3	0.4	0.5	0.6
Current density	A/mm ²	7500	7125	6750	6375	6000	5625	5250
Total wire length	m	1	2	4	6	8	11	15
Total wire resistance	Ohm	0.00	0.00	0.00	0.00	0.00	0.00	0.00
Required power	W	0.00	0.00	0.00	0.00	0.00	0.00	0.00
Total wire weight	Kg	0.004	0.009	0.018	0.029	0.041	0.054	0.070
Winding layers		1	1	1	1	1	1	1

Table 2: Coil characteristics for NbTi

Comparing the currents density flowing in the copper coil and in the NbTi coil, we see that there is a difference of three order of magnitudes; the same reduction holds for the number of turns and, therefore, for the coil's volume and weight. Moreover, the peculiar feature of SC materials of having no resistivity to flowing currents means no power is required, which, in turn, means a dramatic reduction in mass and volume of the power processing unit (PPU).

Even if the density of the currents flowing in the SC coil were to be well under the critical value, it would be still advantageous to use it, as seen in the following table:

B field	T	0.05	0.1	0.2	0.3	0.4	0.5	0.6
Current density	A/mm ²	300	300	300	300	300	300	300
Total wire length	m	21	42	85	127	170	212	255
Total wire resistance	Ohm	0.00	0.00	0.00	0.00	0.00	0.00	0.00
Required power	W	0.00	0.00	0.00	0.00	0.00	0.00	0.00
Total wire weight	Kg	0.102	0.204	0.409	0.613	0.817	1.022	1.226
Winding layers		1	1	2	3	4	5	6

Table 3 : Coil characteristics for NbTi for "low" current densities

SC materials can be used to produce high B field with low weight and volume penalties, as can be seen in the next table.

B field	T	1	2	3	4	5	6	7
Current density	A/mm ²	4000	3525	3075	2625	2175	1725	1050
Total wire length	m	32	72	124	194	293	443	849
Total wire resistance	Ohm	0.00	0.00	0.00	0.00	0.00	0.00	0.00
Required power	W	0.00	0.00	0.00	0.00	0.00	0.00	0.00
Total wire weight	Kg	0.153	0.348	0.598	0.934	1.409	2.132	4.087
Winding layers		1	2	3	5	7	11	20

Table 4: Coil characteristics for NbTi for high B field

The next figures show some of the results reported in the above tables.

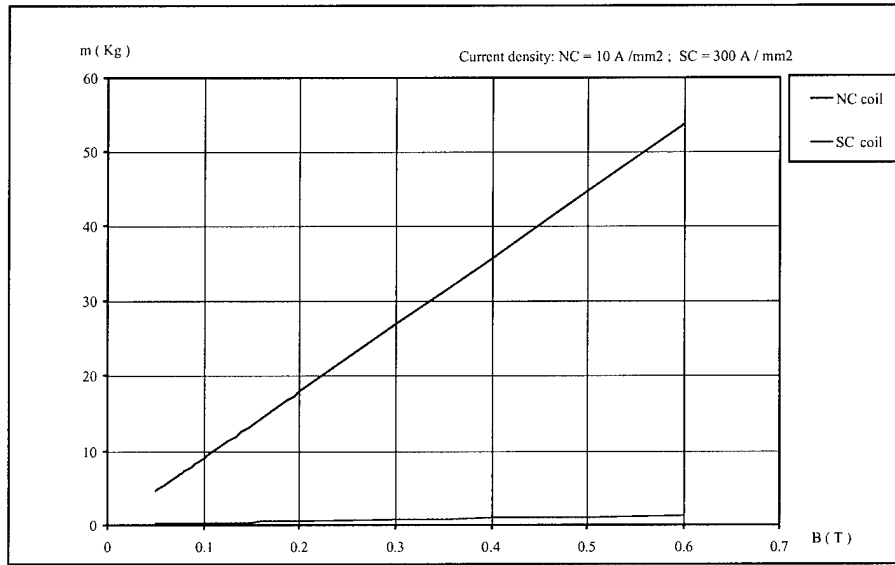


Figure 5: Comparison of coil weights relative to the B field generated

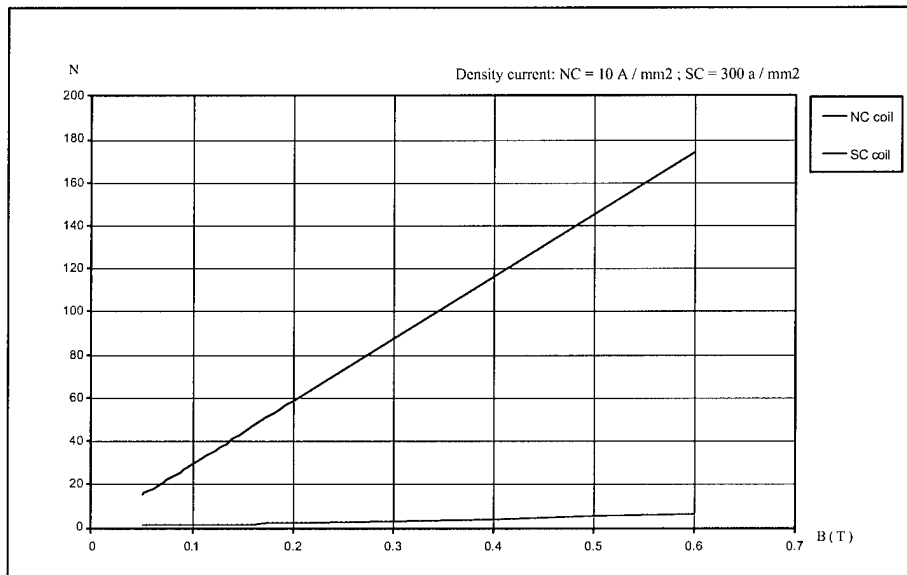


Figure 6: Comparison of coil winding layers relative to the B field generated

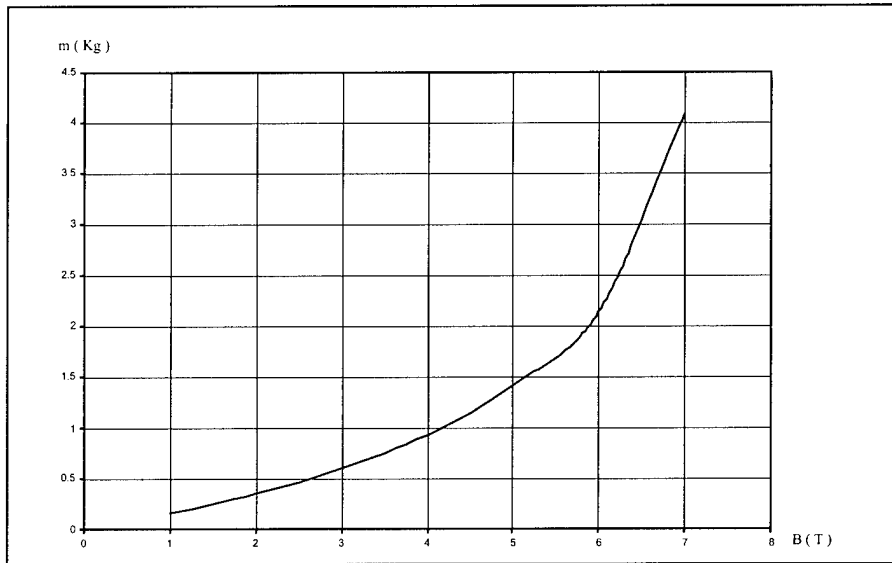


Figure 7: SC coil weight relative to the B field generated

High B fields generated by SC coils increase the Lorentz force ($F = J \times B$) exploited as thrust. The next figure report an evaluation of the thrust generated using a B field in the range of 0 ÷ 7 T. To perform the calculations, the following assumptions have been made:

1. Arc current $I = 400$ A [Giucci, 1999].
2. Anode – cathode distance $l = 0.02$ m [Sovey and Manteniaks, 1991].
3. Gas (Ar) flow rate $m = 100$ mg/s [Giucci, 1999].

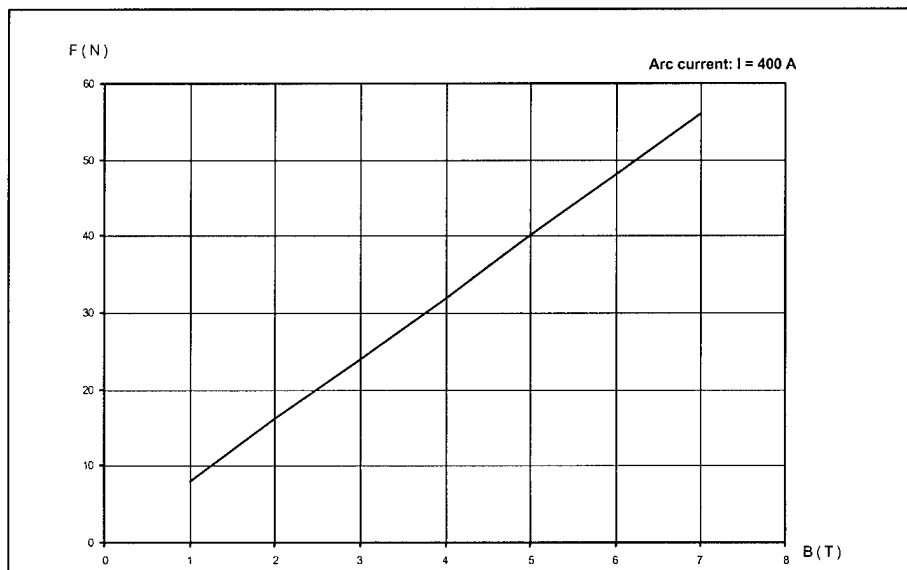


Figure 8: Thrust as function of the B field generated by a SC coil

In the next figure the corresponding I_{sp} is reported.

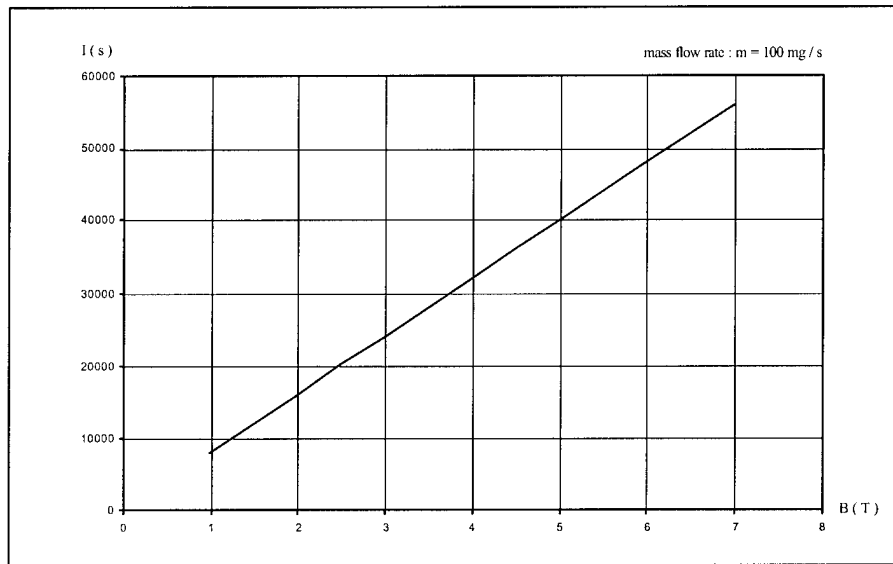


Figure 9: I_{sp} as function of the B field generated by a SC coil

The following conclusions can be drawn:

1. With a current $I = 400$ A and a magnetic field $B = 7$ T, a Lorentz force $F = 56$ N can be achieved; in this case the SC coil would weigh about 4 Kg. With a Cu coil weighing the same, a magnetic field $B = 0.05$ T would be obtained, with a corresponding Lorentz force $F = 0.4$ N.
2. I_{sp} up to 56000 s can be achieved.
3. This performance can be obtained with relatively “low” currents ($I = 400$ A), with a corresponding reduction in the cathode erosion life.

4 - Low power scaling of SC coils – equipped Hall thrusters

Electric thrusters in the medium – high class power (> 500 W) require a power supply mass that can easily vanish the advantages of using these propulsion systems. Therefore scaling of power (< 500 W) in Hall thrusters without excessive penalties in engine performance (e.g., in the range $I_{sp} = 1500$ s, efficiency = 50 %), is a prime concern.

Power can be downscaled by reducing either the discharge voltage U_d and/or the discharge current I_d ($P = U_d \cdot I_d$). Now considering the specific impulse $I_{sp} = \eta_p v_i / g$ (s) in which, $v_i \propto U_a$ is the average ion velocity ($U_a \sim U_d$ is the voltage drop in the acceleration region), if the discharge voltage is reduced I_{sp} will be lower. Moreover $I_d \propto \dot{m}$: therefore reducing I_d will lower \dot{m} , which, in turn for a given thruster geometry, will negatively affect I_{sp} and efficiency. In fact, considering the mean free path for ionisation:

$$\lambda_i \propto \frac{S}{\eta_p \dot{m}}$$

where S is surface cross sectional area of the channel and η_p is propellant utilization,

reducing l_a (and thus m) will increase λ_i . Now in order to obtain high propellant utilization, it must be $\lambda_i < L$, where L is the channel length; even if we assume at first that η_p is not changed, when the mass flow rate is reduced λ_i increases, and the probability of atom ionisation drops, resulting in lower propellant utilization. This will have a negative effect on engine performance (i.e., I_{sp} and efficiency).

A way to keep λ_i constant (thus without penalties in engine performance) while reducing m , is to scale the thruster geometry (i.e. its scale S). Geometrical scaling of the thruster must prevent power losses, in order to keep the overall efficiency high. These losses depend mainly on ions hitting the wall (and recombining) in the accelerating region; therefore the fraction of the ion flux that leaves the channel without hitting the wall could be considered as a measure of efficiency. This parameter depends primarily on two factors: the angle under which the accelerated ions "see" the exit, scaling as h/l_a , and the dispersion in the direction of the accelerated ions, estimated to go as

$[k T_e / (eU_a)] \cdot (l_a/h)$. As a result the fraction of ions that are accelerated without hitting the wall scales as: $[(eU_a)/k T_e] \cdot (h/l_a)^2$. From this expression it can be seen that the losses depend mainly on two factors:

- 1 - Ratio between channel width and accelerating region length: $r = \frac{h}{l_a}$.
- 2 - Electron temperature: $T_e \propto \frac{m_e U_a^2}{l_a^2 B^2}$.

Therefore, in order to prevent power losses, the following considerations apply:

- from item 1 it can be seen that if the width of the channel, h , is reduced the length of the accelerating region l_a must be reduced correspondingly.
- from item 2 it can be seen that to keep the electronic temperature constant while downscaling the geometry, the B field must go as $\frac{1}{l_a}$, which means that while downscaling the geometry, B must be increased.

Increasing of the B field is constrained by limits imposed by weight and size, if copper is the conducting material. To see it we can compare the volume of the engine and the volume of the coil needed to generate the B field when we proceed with the scaling. In scaling the engine the following relationships hold:

$$V_k = K^3 V_{fs} \quad (1)$$

where V_k scaled volume, V_{fs} full scale volume, K scaling factor ($K < 1$).

For the coil volume:

$$V_{coil} = l_w A_w \quad (2)$$

with A_w coil wire section.

$$l_w = \frac{\pi D_{coil} L_{coil}}{\mu_o I_{coil}} B \quad \text{: coil wire length} \quad (3)$$

Now we have:

$$B \propto \frac{1}{l_a} \quad (4)$$

if we scale the engine:

$$h_k = K h_{fs} \quad (5)$$

Therefore:

$$B_k = \frac{1}{K} B_{fs} \quad (6)$$

Assuming $D_{coil} = \text{const.}$, $L_{coil} = \text{const.}$, $I_{coil} = \text{const.}$, finally we have:

$$(V_{coil})_K = \frac{1}{K} (V_{coil})_{fs} \quad (7)$$

This relation is valid for both NC and SC materials; the only difference is the initial value for $(V_{coil})_{fs}$. In fact, considering Table 1 and Table 2, which report, among other parameters, the total wire length needed to produce the corresponding B field, it can be seen that, whatever the B field, the volume of the SC coil material will always be about 640 times smaller than that of the NC coil material.

Now, to see the limit imposed on scaling if copper is to be used to produce a B field, we can consider a THT – series Hall thruster (Tahara et al., 1999), reported in Figure 10.

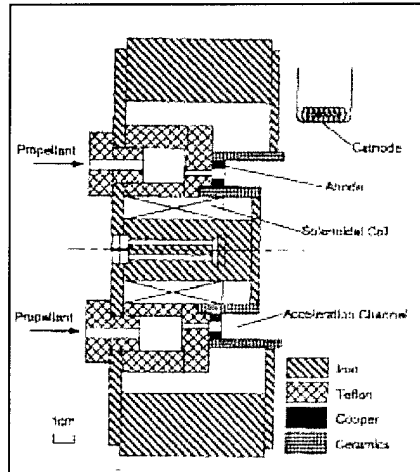


Figure 10: Cross section of THT – series Hall Thruster

Coil volume V_{coil} and casing volume V_{casing} are:

$$V_{coil} = 1.45 \cdot 10^{-5} \text{ m}^3$$

$$V_{casing} = 5.78 \cdot 10^{-5} \text{ m}^3$$

The results of applying the scaling relations for copper and NbTi are reported in Figure 11. This figure shows how the use of NC material to generate a B field sets a limit on scaling the engine, while, as a first instance, the use of a SC material does not affect the scaling.

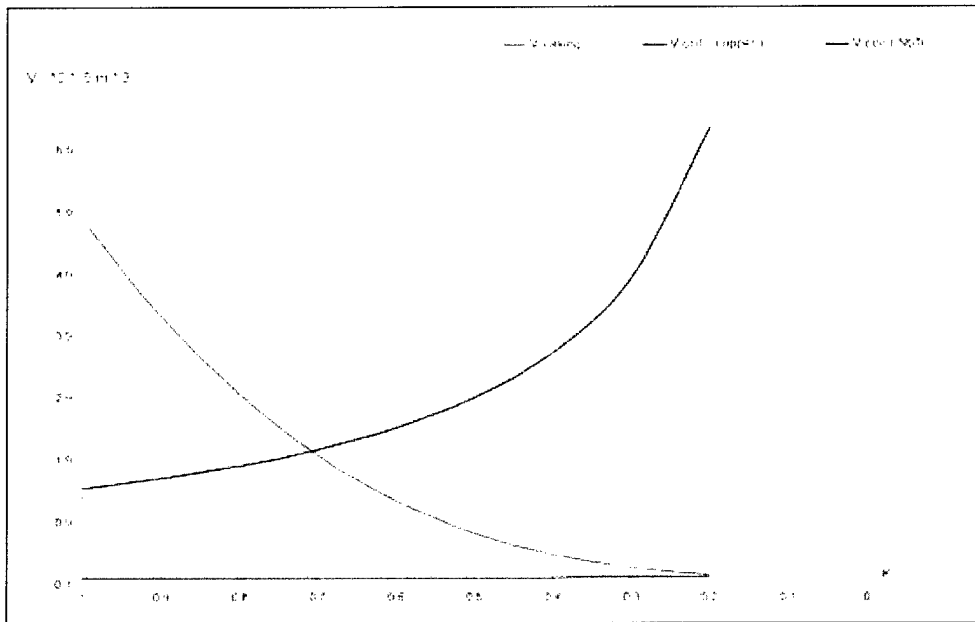


Figure 11: Visualization of scaling relations for casing and coil volume

To conclude: the use of SC materials instead of NC material such as copper to generate a B field in Hall thrusters, can be exploited to conveniently scale engines. In this way it is possible to obtain “low” power engines ($< 500 \text{ W}$) without excessive penalties in their performance, and also to save weight, due to the reduction of power supply mass and coil mass as well. Moreover, increasing the B field needed to perform scaling without penalties can be exploited advantageously in terms of thrust, as can be seen considering the Lorentz force: $\vec{F} = \vec{J} \times \vec{B}$.

5 - Stresses on magnetic coils

A solenoid is subjected to a Lorentz force due to the interaction between the B field generated by the flowing current and the current itself. As a consequence stresses in the coil tend to burst it radially and crush axially.

For the hoop stress the following expression apply [Montgomery, 1969]:

$$s_t = \frac{H I a_1}{l t} c \quad (8)$$

with H in oersteds, I in amperes, and s_t in kilograms per square centimeters for $c = 10^{-6}/9.8$.

The field is assumed to be produced by the current per unit length l, therefore the following relation between the current and the H field apply:

$$\frac{I}{l} = \frac{H}{(4\pi/10) \cos\theta} \quad (9)$$

in this expression θ is the angle between solenoid axis and lines drawn from origin to various points in the end plane of solenoid. In Figure 12 a schematic of the solenoid is reported.

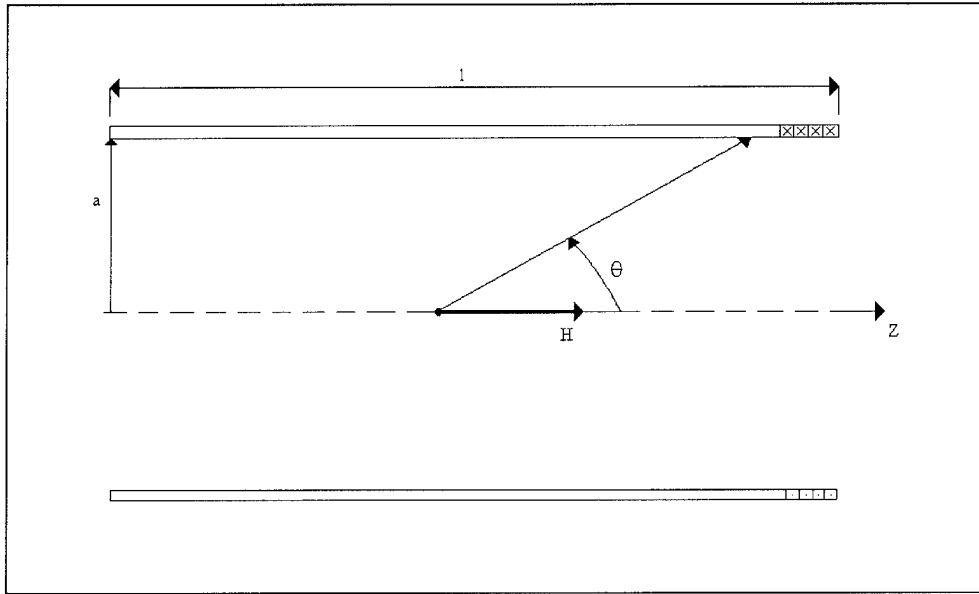


Figure 12: Schematic of the solenoid

For a solenoid whose length is much greater than its diameter $\cos \theta \sim 1$; substituting in the stress expression the following relation holds:

$$s_t = 4 \cdot 10^{-8} H^2 \frac{a_l}{t} \quad (10)$$

In this expression the dependence of the stresses on coil geometry (i.e., the ratio a/t), and on H^2 can be noticed. Now the magnitude of the stress on a magnetic coil can be easily calculated; if we consider again a coil having the following features, typical of satellite applications:

- Length: $L = 0.1 \text{ m}$
- Diameter: $D_t = 0.14 \text{ m}$
- Wire diameter: $d_w = 1 \text{ mm}$

in the range of B field as in Table 4, page 6, the corresponding stress acting on the material is reported in the next table.

B (T)	s_t (MPa)
1	28
2	112
3	252
4	448
5	700
6	1008
7	1372

Table 5: Stress on magnetic coil

Considering the brittle nature of SC materials, jackets are needed in order to sustain the stresses. The requirements in the choice of jacket materials is on weight as well as ultimate strength of the material; therefore even though steel could be a suitable jacket material due to the high ultimate strength, its specific weight is too penalizing for satellite applications. A possible solution could be the use of composite materials, such as Carbon - Carbon; In Figure 13 typical properties of carbon composite materials are reported: it can be seen that at 0 °C (273 K) the ultimate tensile strength for these materials range from 400 to 700 MPa.

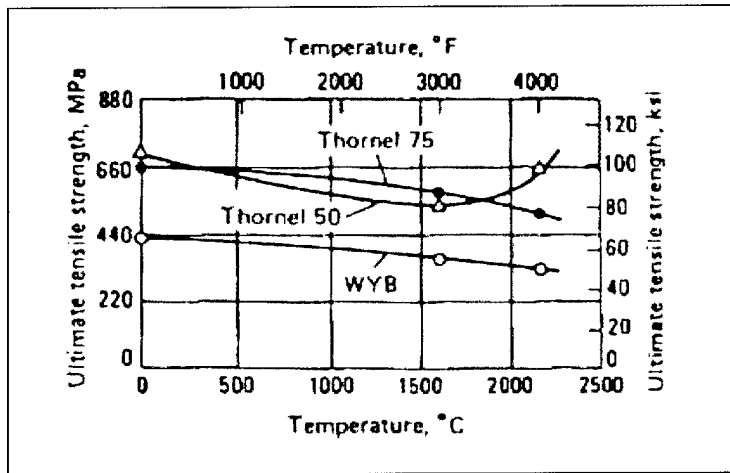


Figure 13: Typical properties of composite materials

Now for stress on the jacket the following relation apply:

$$s = \frac{P \cdot D}{2 t_j} \quad (11)$$

where P is the pressure, D the diameter and t_j jacket thickness; for a given pressure and diameter, the stress on the jacket depends on its thickness. For ease of calculations a mean diameter $D = 0.14\text{m}$ has been considered. The pressure acting on the jacket is given by the following expression:

$$P = \frac{2 s_t t}{D_t} \quad (12)$$

Therefore for the jacket thickness the following expression apply:

$$t_j = \frac{s_t t}{s} \quad (13)$$

To perform the calculations for the jacket thickness, the ultimate strengths of the three composite materials reported in Figure 13, at 0 °C (273 K), have been considered; therefore:

- WYB $s \sim 440 \text{ MPa}$
- Thornel 75 $s \sim 660 \text{ MPa}$
- Thornel 50 $s \sim 700 \text{ MPa}$

The SC stresses (s_t) considered are those plotted in Table 5, for the B field varying between 1 and 7 T; wire thickness is $t = 1\text{mm}$.

Table 6 and Figure 14 report the jacket thickness (in mm) for the three different materials.

B (T)	s_t	WYB	Thornel 75	Thornel 50
1	28	0.064	0.0424	0.04
2	112	0.255	0.17	0.16
3	252	0.573	0.382	0.36
4	448	1.02	0.679	0.64
5	700	1.591	1.06	1
6	1008	2.291	1.53	1.44
7	1372	3.118	2.079	1.96

Table 6: Jacket thickness (in mm)

Therefore, from the above consideration it can be seen that Carbon composite could be thought as suitable jacket materials in the aforementioned configuration with a B field ranging between 1 and 7 T.

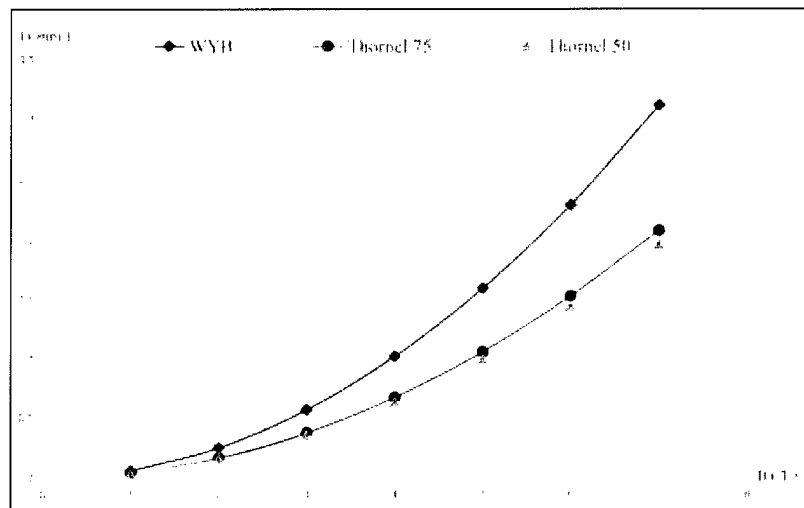


Figure 14: Jacket thickness vs. applied B field

6 - Cooling systems for SC coils

In order to work properly, SC coils must work below the SC material critical temperature; therefore is important to realize a cooling system for space applications, that must match the following conditions:

- High reliability.
- Automatic operation.
- Low power.
- Capability to work in a microgravity environment; for certain applications, however, it must work while accelerating.

- Capability to ensure proper temperature conditions for the whole mission time.
- Compactness and low weights required.

Cryogenic techniques applied to SC coil cooling can be derived directly from the field of “space cryogenics” utilized onboard of satellites to cool some of their components, such as optical instrumentation.

Until recently the preferred technique consisted in having onboard the satellite a “cold bath” for the systems to be cooled; although this system is simple, its limits are due mainly by the volume, weight and operational time. As an example the system employed on the ISO (Infrared Space Observatory), contained 2000 litres of liquid helium to ensure an operational time of 2 years. This meant a volume $\sim 2 \text{ m}^3$ and a weight of about 2 tons, for a mission limited in time. Therefore new concepts in “space cryogenics” had to be developed, in order to shrink volume and weight of the cooling system(s); these are based mainly on manufacturing the cold onboard, and can be as follows:

- Passive cooling systems.
- Active cooling systems.

Passive cooling systems consist in radiating heat to space, without energy requirement by the system. This technique has the advantage of simple operability conditions, low volume and weight, long operation time. On the other side there is a limitation on the minimum temperature (about 70 K), on satellite configuration and on orbit characteristics.

Active cooling systems are based on a refrigerating thermodynamical cycles. These systems can be classified, depending on the thermodynamical cycle, as:

- a - Systems in which external work is not required (Joule – Thomson refrigerators).
- b - Systems in which external work is required (Stirling refrigerators).

Coolers based on the latter systems are able to provide the needed refrigeration with a reasonable demand in power input, and for a life time of 10 years. Considering as refrigerating fluid for a HTSC material (critical temperature $T_c > 120 \text{ K}$), Nitrogen (boiling temperature $T_b = 77 \text{ K}$), available commercial active coolers are able to keep the fluid at the required temperature for a minimum life time of 5 years without excessive power requirements, as can be seen in the next table.

Program/ Sponsor	PSC/ Philips Lab	PSC/ Philips Lab	EOS 80 K/ NASA GSFC	EOS 30 K/ NASA GSFC	COOLAR	AIRS/ NASA JPL
Refrig. Design	1 Stage Stirling	1 Stage Stirling	1 Stage Stirling	2 Stage Stirling	Mech. J-T 2 Stage	1 Stage Stirling
Vendors	LMSC/HAC	TRW	HAC/LMSC	Ball	Ball	TBD
Rqmt's	2 W @ 60 K 40 W 10 years	1 W @ 150 K 15 W 10 years	0.8 W @ 80 K 30 Lbs 5.7 years	0.3 W @ 30 K 80 W 40 Lbs 5.7 years	3.5W @ 65K 300 W 150 Lbs 5 years	1W @ 55K 100 W 5.7 years

Table 7: Basic features of different commercial cryogenic systems

A last consideration is on the mass budget for the system; the total weight for the system is only about 11 Kg; with such a system the thruster is able to produce a variable thrust in the range of

10 ÷ 20 Newton, depending on the magnetic B field and the discharge current; a copper coil weighing the same would produce a thrust of 1 N at best. The results are reported in the following table.

Dewar	0.6 Kg		
Liquid Nitrogen	0.9 Kg		
Cooling System	7 ÷ 8 Kg		
Superconducting + Mechanical support	1 ÷ 2 Kg	B field	Thrust
Superconducting Solution (total mass)	~ 11Kg	5 T	10 ÷ 20 N
Traditional Copper Solution	~ 11Kg	0.1 T	0.4 ÷ 1 N

Table 8: Total mass budget

7 – Specific development topics

Issues to be considered in developing Hall thrusters are the following:

7.1 Plume divergence

Plume divergence could have effects on satellite hardware, e.g., solar arrays, antennas, etc, and on surrounding environment as in the case of constellation satellite systems: therefore it is important to determine the parameters to be optimised in order to reduce the divergence. Figure 15 shows the experimental curve of plume divergence vs. power for the X-40 prototype Hall thruster, while on Table 9 the corresponding optimised parameters are reported [Belikov et al., 1999].

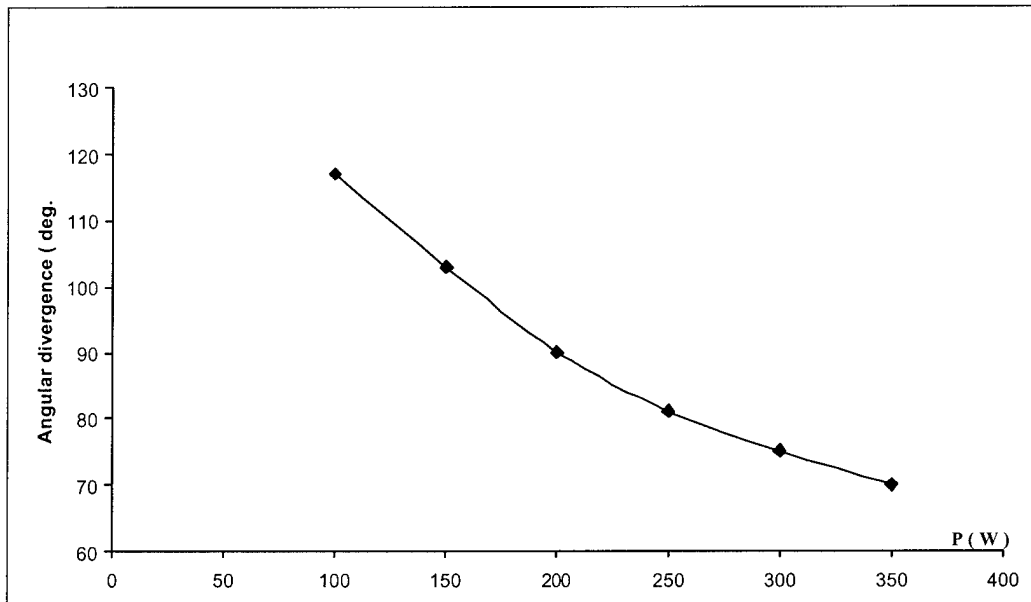


Figure 15 : Plume divergence vs. power

Discharge power, w	Discharge voltage, v	Discharge current, a	Anode flow rate, mg/s	Thrust, mn	Specific impulse, s	Efficiency, %
100	150	0.67	0.74	7.43	1020	37
200	1961	1.03	1.08	14.5	1370	48
300	230	1.30	1.35	20.1	1518	50
350	250	1.40	1.45	22.9	1598	51

Table 9: Optimal operation mode of X-40

Because of the higher velocity/power, increasing power leads to more coherent “stiffer” plasma jets. In this sense higher Isp due to use of SC and higher B field should be likely beneficial, with lower angular spreading/divergence.

7.2 B fields interference

High B fields in thrusters could interfere, in principle, with electronic satellite onboard systems, e.g., data acquisition and transmission. At the moment, due to lack of information, further study is needed.

8 - Overview for future applications

In the preceding sections the benefits that could be produced by SC coils in EP have been presented. Here an overview on possible applications is reported.

8.1 Low Power Hall Thrusters

If high B fields are possible, as it seems to be the case with SC coils, there is the possibility of scaling Hall thrusters for efficient operation at low power $O(10)$ to $O(100)$ W. The scaling could lead to the development of linear Hall thrusters. This type of thrusters are characterized by compact packaging, allowing, if needed, the implementation of multiple arrays of thrusters. The stacked system of thrusters could be used to maintain operation at maximum efficiency: this can be achieved by turning the thrusters on and off in order to reach wanted thrust level, instead of changing the operating point of a single thruster [Schmidt et al, 1999]. In Figure 16 a schematic of the linear Hall thruster is reported.

Application of SC material for generating high B field will always lead to more compact magnetic coils compared to NC coils, for a given B field value; compactness can be exploited, among other factors, to better target the B field in the thruster. In fact the axial variation of the magnetic field has a large impact on discharge performance. It is desirable to have a sharp peaked magnetic field near the exit of the acceleration channel, with a distribution width narrower than the channel depth. In this way reduction in thruster efficiency will be prevented [Schmidt et al, 1999].

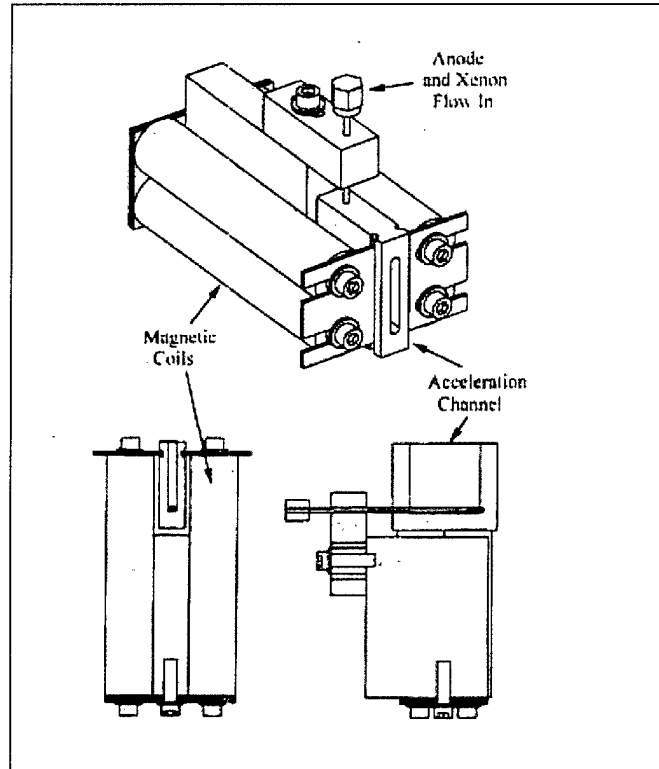


Figure 16: Cross section and isometric view of the linear Hall thruster

8.2 High Power Hall Thrusters

High power electric thrusters represent the key point in future manned space explorations. Studies for the development of high power Hall thrusters (e.g., $P \sim 25 \div 50$ KW) are under way in Russia [Garkusha et al., 1999] as well in USA [Dunning and Sankovic, 1999].

Investigations with a laboratory Hall thruster, the SPT100 – ML, has demonstrated that an increase in the magnetic field strength lead to an increase in thruster performance [Béchu et al, 1999]. In the next figures the results for thrust, specific impulse and efficiency, are reported.

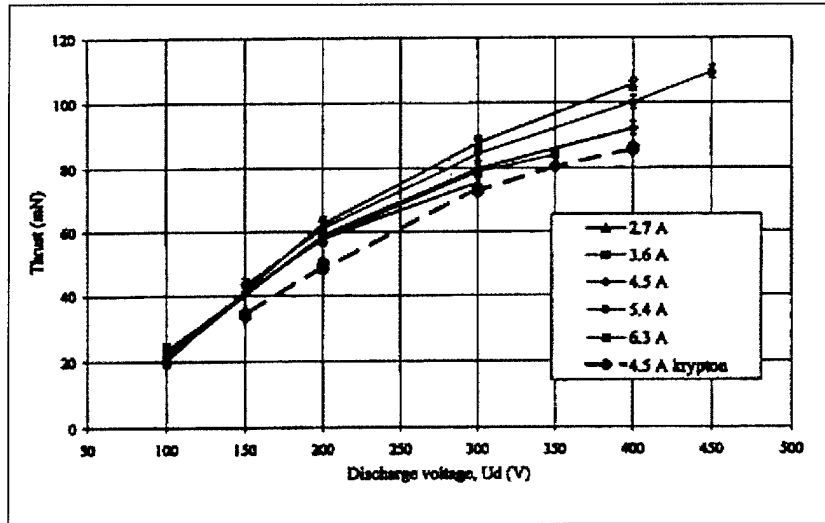


Figure 17: Thrust as function of discharge voltage.

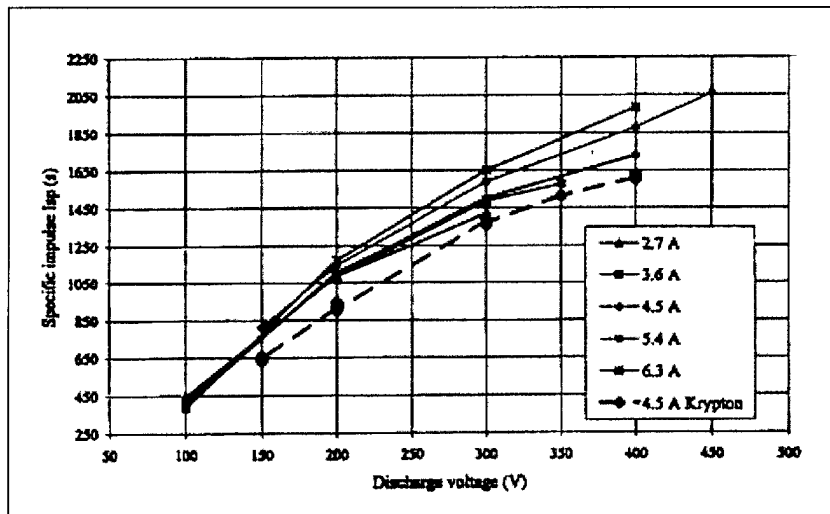


Figure 18: Isp as function of discharge voltage.

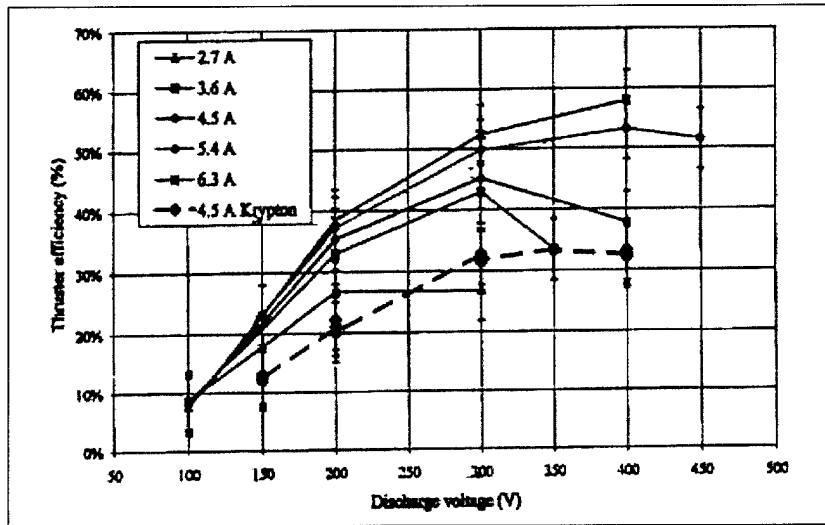


Figure 19: Thruster efficiency as function of discharge voltage.

The above conclusions could be extrapolated for high power thrusters; therefore high B fields could improve high power Hall thrusters performance. In this sense SC coils could be usefully applied to generate high B field, without the typical difficulties that would be encountered with NC coils (e.g., power losses due to Joule heating).

8.3 MPD Thrusters

High B fields can be exploited in thrusters which are based on the Lorentz force. A class of such thrusters is the MHD accelerators; for this type of accelerators two configurations are possible: Crossed - field Faraday accelerators and Hall current accelerators [Li et al., 2000]. Figure 20 and Figure 21 show a schematic of the two configurations.

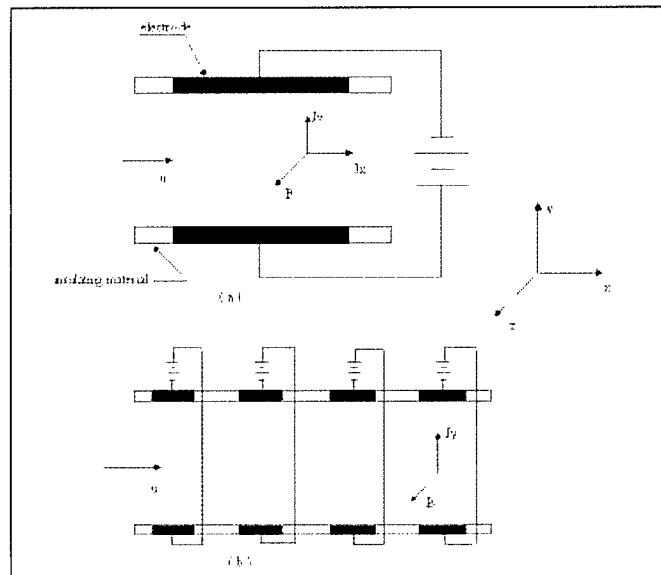


Figure 20: Crossed-field Faraday accelerators. (a) Continuous electrodes (b) Segmented electrodes

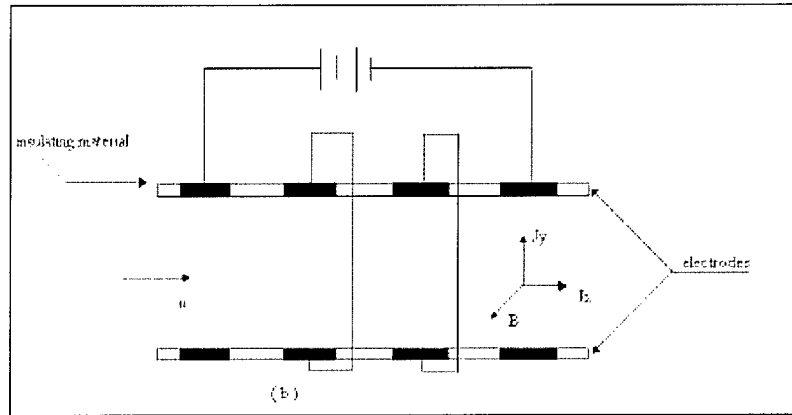


Figure 21: Hall current accelerator with constant area

The basic thrust relations for the two configurations are the following [Hawk et al., 2000]:

1. Crossed – field Faraday accelerator:

$$F_x = s u B_z^2 [K_f - 1] \quad (1)$$

$$K_f = \frac{E_y}{u B_z} : \text{loading factor}$$

$$\eta_f = \frac{1}{K_f} : \text{efficiency}$$

2. Hall current accelerator:

$$F_x = \frac{s u B_z^2}{1 + (\omega\tau)^2} [(\omega\tau)^2 K - 1] \quad (2)$$

$$K = \frac{E_x}{(\omega\tau) u B_z} : \text{loading factor}$$

$$\eta = \frac{(\omega\tau)^2 K - 1}{(\omega\tau)^2 K (K + 1)} : \text{efficiency}$$

In both cases it can be seen that, for a fixed loading factor, thrust increases with B^2 . If power is not the primary limitation, the loading factor (and thus efficiency) can be kept at an optimum value while scaling up the B field. Therefore, high thrust values can be achieved with the use of SC coils (high B field), in high power MHD accelerators.

8.4 Conclusions

From this short overview it appears possible to use SC for a type of Hall as well for MPD thrusters. Thinking of a possible demonstration of this technology, a near term application would be probably easier for a new high power MPD thruster. In fact, one of the major objections/problems to MPD

(the high power loss due to high B, high current coils) would be greatly reduced or altogether eliminated, leaving all the power available for thrust generation. In this sense MPD thrusters with SC coils need to be re-assessed, in view of the potential enlarged field of application due to superconductivity.

References

- Ashkenazy J., Raites Y., Appelbaum G., (1997), "Low Power Scaling of Hall Thrusters", Second European Spacecraft Propulsion Conference, 27 – 29 May 1997, ESTEC, Noordwijk, The Netherlands, pp. 455 – 460.
- Béchu, S., Pérot, C., Gascon, N., Lasgorceix, P., Hauser, A., Dudeck, M., (1999), "Operating Mode Investigation of a Laboratory Stationary Plasma Thruster", AIAA Paper 99 – 2567, presented at 35th AIAA/ASME/SAE/ASEE Joint Propulsion Conference, Los Angeles, Ca., June 1999.
- Belikov, M. B., Gorshcov, O. A., Rizakhanov, R. N., Shagayda, A. A., 1999, "Hall Type Low- and Mean-Power Thrusters Output Parameters ", AIAA Paper 99 – 2571, presented at 35th AIAA/ASME/SAE/ASEE Joint Propulsion Conference, Los Angeles, Ca., June 1999.
- Bishop, D. J., Gammel, P. L., Huse D. A., " La Resistenza nei Superconduttori ad alta Temperatura", *Le Scienze* (Scientific American Italian Edition), n° 296, April 1993.
- Bruno, C., and Czysz, P.A., (1998), "An Electro-Magnetic-Chemical Hypersonic Propulsion System", AIAA Paper 98-1582.
- Bruno, C., and Giucci, S., (1999), "Cryogenic Technology to Improve Electric Thrusters", Paper IAF-99-S.4.04, presented at the 50th IAF Congress, Oct. 4-8, 1999, Amsterdam.
- Choueiri, E.Y., (1999), "Overview of U.S. Academic Programs in Electric Propulsion", AIAA Paper 99 – 2163, presented at 35th AIAA/ASME/SAE/ASEE Joint Propulsion Conference, Los Angeles, Ca., June 1999.
- Christen, D., (1998), "Current limits to wire technology", *Nature*, Vol. 392, pp. 862-863.
- Connolly D. J., Bishop A. R., Seikel G. R., (1971), "Test of Permanent Magnet and Superconducting Magnet MPD Thrusters", AIAA Paper 71 – 696, presented at AIAA/SAE 7th Propulsion Joint Specialist Conference, Salt Lake City, Utah, June 1971.
- Dario, P., Carrozza, M.C., Fenu, A., and Mango, A., (1998), FUSARET: Future Satellite Architecture with Emerging Technologies", ESA-ESTEC Contract No. 12755/98/NL/MV, Final Report to ESA-ESTEC, April 1998.
- Dunning, J., Sankovic, J., (1999), " NASA's Electric Propulsion Program", AIAA Paper 99 – 2161, presented at 35th AIAA/ASME/SAE/ASEE Joint Propulsion Conference, Los Angeles, Ca., June 1999.
- Europa Metalli (1998), Superconductors Division, "Internal Tin Nb₃ Sn Superconducting Wire", Technical Data Sheet, Europa-Metalli SpA, 55052 Fornaci di Barga (Lucca), Italy.

- Garkusha, V., Lukiaschenko, V., Semenkin, A., Tverdokhlebov, S., Kim, V., Popov, G., Maslennikov, N., Murashko, V., (1999), "Modern Status of Hall Thrusters Development in Russia", AIAA Paper 99 – 2157, presented at 35th AIAA/ASME/SAE/ASEE Joint Propulsion Conference, Los Angeles, Ca., June 1999.
- Garre', R., (1998), Europa Metalli-LMI R&D Director, personal communication.
- Giucci, S., (1999), "Propulsione satellitare: linee di tendenza attuali e applicazioni future della superconduttività", Mechanics and Aeronautics Department Thesis, University of Rome "La Sapienza", Rome, Italy (in Italian).
- Grant, P. M., (2000), "Currents Without Borders", Nature, Vol. 407, pp. 139 - 141, 14 Sept. 2000.
- Hammerl G., et al, (2000), "Enhanced Supercurrent Density in Polycrystalline $YBa_2Cu_3O_{7-d}$ at 77 K from Calcium Doping of Grain Boundaries", Nature, Vol. 407, pp. 162 - 164, 14 Sept. 2000.
- Jahn, R. G., (1968), "Physics of Electric Propulsion", McGraw – Hill Series in Missile and Space Technology, New York, 1968.
- Jahn, R. G., and Choueiri, E. Y., (2000), "Electric Propulsion", Article in the Academic Press Encyclopedia of Physical Science and Technology", to appear in 2000.
- Li, Z., Jones, J. E., Hawk, C.W., (1999), "Experimental Study of Microwave Plasma MHD Accelerators", AIAA Paper 2000 - 3882, presented at 36th AIAA/ASME/SAE/ASEE Joint Propulsion Conference, Huntsville, AL, July 2000.
- Montgomery, D. B.,(1969), "Solenoid Magnet Design", Wiley - Interscience, Wiley & Sons, New York, 1969.
- Randolph, T., (1999), "Overview of Major U.S. Industrial Programs in Electric Propulsion", AIAA Paper 99 – 2160, presented at 35th AIAA/ASME/SAE/ASEE Joint Propulsion Conference, Los Angeles, Ca., June 1999.
- Reed, B., and Sovey, S., (1988), "The Use of High Temperature Superconductors in Magnetoplasmadynamic Systems", in: Proc. of the 2nd Annual Conference on Superconductivity and Its Applications, April 18-20, 1988, ed. by S. Kwok and T. Shaw, Elsevier Science Publishing Co., New York, 1988.
- Saccoccia, G., (1999), "European Electric Propulsion Activities and Programmes", AIAA Paper 99 – 2158, presented at 35th AIAA/ASME/SAE/ASEE Joint Propulsion Conference, Los Angeles, Ca., June 1999.
- Scaramuzzi, F., (1996), "Active Cooling Systems", paper presented at the "Infrared Space Interferometry Workshop", organized by: Universidad Autonoma de Madrid, Laboratorio de Astrofisica Espacial y Fisica Fundamental, Instituto de Astrofisica de Andalucia, Toledo, Spain, 11 – 14 March 1996.
- Schmidt, D.P., Meezan, N.B., Hargus, W.A. Jr., Cappelli, M.A., (1999), "Operating Characteristics of a Linear Hall Thruster with an Open Electron – Drift", AIAA Paper 99 – 2569, presented at 35th AIAA/ASME/SAE/ASEE Joint Propulsion Conference, Los Angeles, Ca., June 1999.

Scortecci, F., Capecchi, G., Andrenucci, M., Mei, G., and Garre', R., (1993), "Development of a Superconducting Electromagnet for Applied Field Arcjet Thrusters", Paper IEPC-93-119, presented at the 23rd International Electric Propulsion Conference, Sept. 1993, Seattle.

Sovey, J. S., and Manteniaks, M. A., (1991), "Performance and Lifetime Assessment of Magnetoplasmadynamic Arc Thruster Technology", J. Propulsion and Power, Vol. 7, No 1, Jan – Feb 1991, pp 71-83.

Spores, R.A., Birkan, M., (1999), "The USAF Electric Propulsion Program", AIAA Paper 99 – 2162, presented at 35th AIAA/ASME/SAE/ASEE Joint Propulsion Conference, Los Angeles, Ca., June 1999.

Tahara H., Nikai Y., Yasui T., Yoshikawa T., (1999)," Hall Thruster Research at Osaka University", AIAA Paper 99 – 2570, presented at 35th AIAA/ASME/SAE/ASEE Joint Propulsion Conference, Los Angeles, Ca., June 1999.

Tahara H., Nishida M., (1999), "Overview of Electric Propulsion Activity in Japan", AIAA Paper 99 – 2159, presented at 35th AIAA/ASME/SAE/ASEE Joint Propulsion Conference, Los Angeles, Ca., June 1999.

Faculty of Engineering, University of Bologna, Italy, website:
www.die.ing.unibo.it